



# A rigorous and realistic Shape From Shading method and some of its applications

Emmanuel Prados, Olivier Faugeras

## ► To cite this version:

Emmanuel Prados, Olivier Faugeras. A rigorous and realistic Shape From Shading method and some of its applications. RR-5133, INRIA. 2004. <inria-00071450>

**HAL Id: inria-00071450**

**<https://hal.inria.fr/inria-00071450>**

Submitted on 23 May 2006

**HAL** is a multi-disciplinary open access archive for the deposit and dissemination of scientific research documents, whether they are published or not. The documents may come from teaching and research institutions in France or abroad, or from public or private research centers.

L'archive ouverte pluridisciplinaire **HAL**, est destinée au dépôt et à la diffusion de documents scientifiques de niveau recherche, publiés ou non, émanant des établissements d'enseignement et de recherche français ou étrangers, des laboratoires publics ou privés.

*A rigorous and realistic Shape From Shading  
method and some of its applications.*

Emmanuel Prados — Olivier Faugeras

**N° 5133**

March 2004

THÈME 3



*R*  
*apport*  
*de recherche*



## **A rigorous and realistic Shape From Shading method and some of its applications.**

Emmanuel Prados\* , Olivier Faugeras†

Thème 3 — Interaction homme-machine,  
images, données, connaissances  
Projet Odyssée

Rapport de recherche n° 5133 — March 2004 — 20 pages

**Abstract:** This article proposes a rigorous and realistic solution of the Lambertian Shape From Shading (SFS) problem. The power of our approach is threefolds. First, our work is based on a rigorous mathematical method: we define a new notion of weak solutions (in the viscosity sense) which does not necessarily requires boundary data (contrary to the work of [28, 27, 26, 4, 11]) and which allows to define a solution as soon as the image is (Lipschitz) continuous (contrary to the work of [22, 9]). We prove the existence and uniqueness of this (new) solution and we approximate it by using a provably convergent algorithm. Second, it improves the applicability of the SFS to real images: we complete the realistic work of [26, 30], by modeling the problem with a pinhole camera and with a single point light source located at the optical center. This new modelization appears very relevant for applications. Moreover, our algorithm can deal with images containing discontinuities and black shadows. It is very robust to pixel noise and to errors on parameters. It is also generic: i.e. we propose a unique algorithm which can compute numerical solutions of the various perspective and orthographic SFS models. Finally, our algorithm seems to be the most efficient iterative algorithm of the SFS literature. Third, we propose three applications (in three different areas) based on our SFS method.

**Key-words:** Applications of Shape from Shading; real images; Shape from Shading without boundary data, viscosity solutions with state constraints; black shadows; light source located at the optical center; perspective Shape From Shading; “generic” Hamiltonian.

\* <http://www-sop.inria.fr/odyssee/team/Emmanuel.Prados/>

(Odyssée Lab., INRIA/ENS/ENPC, France)

† <http://www-sop.inria.fr/odyssee/team/Olivier.Faugeras/>

(Odyssée Lab., INRIA/ENS/ENPC, France)

## **“Shape-From-Shading”: Une approche réaliste et rigoureuse; exemples d’applications.**

**Résumé :** Cet article propose une solution réaliste et rigoureuse du problème du “Shape-From-Shading” Lambertien. La puissance de notre approche est triple. Tout d’abord, celle-ci est basée sur une méthode mathématique rigoureuse: nous définissons une nouvelle notion de solutions faibles (au sens des solutions de viscosité) qui ne requiert pas nécessairement de données au bord (contrairement aux travaux de [28, 27, 26, 4, 11]) et qui permet de définir une solution dès que l’image est Lipschitzienne (contrairement aux travaux de [22, 9]). Nous prouvons l’existence et l’unicité de cette (nouvelle) solution et nous l’approximons en utilisant un algorithme dont nous prouvons la convergence. Deuxièmement, notre approche augmente l’applicabilité du “Shape-From-Shading”. Nous complétons la modélisation réaliste proposée par [26, 30], en considérant une caméra de type sténopé et une source de lumière ponctuelle disposée au centre optique: cette nouvelle modélisation est très pertinente pour les applications et permet d’obtenir d’excellents résultats sur des images réelles. Notre algorithme permet de plus de traiter des images contenant des discontinuités et des ombres portées. Celui-ci est très robuste aux bruits pixéliques et aux erreurs faites sur les paramètres. Il est aussi générique: i.e. nous proposons un unique algorithme qui peut calculer des solutions numériques des divers modèles de “Shape-From-Shading” orthographiques et perspectifs. Enfin, notre algorithme semble être l’algorithme itératif le plus “performant” de la littérature du “Shape-From-Shading”. Troisièmement, nous proposons trois applications (dans trois domaines différents) basées sur notre méthode.

**Mots-clés :** Applications du Shape from Shading; images réelles; Shape from Shading “sans” condition aux limites, solutions de viscosité avec contraintes d’état; ombres portées; source de lumière au centre optique; Shape From Shading perspectif; Hamiltonien “générique”.

## 1 Introduction

The Shape From Shading (SFS) problem consists in computing the three-dimensional shape of a surface from the brightness variations in a black and white image of that surface. Pioneered by Horn [13] in the 70s, this problem has been central in the field of computer vision since the early days. Nevertheless, because of several reasons, the interest in this problem has slightly decreased at the end of the 90s. First, due to the difficulty of the problem, progress in SFS research is very slow. Second, until recently, the results obtained on real images have been very disappointing. For example, in [34], Zhang et al. acknowledge failure. Third, the various constraints imposed by the existing solutions to the SFS problem limit its applications. In this article, we attempt to change this situation completely and hope to revive the interest of the community for this old problem and its applications.

1. We propose a *new mathematical framework* really adapted to SFS, and allowing to tackle the difficulties of this ill-posed problem (see section 4). It *does not necessarily require boundary data* (as opposed to the somewhat unrealistic work of [28, 27, 26, 4, 11]) and allows to define a solution as soon as the image is only (Lipschitz) continuous (in contrast to the work of Oliensis and Dupuis [22, 9]). Also, in order to approximate these new solutions, we propose a *provably convergent algorithm*, in section 5.
2. We improve the applicability of SFS. In section 2, we propose a *new equation* realistically modeling a simple camera equipped with a flash, or such medical imaging systems as endoscopy. Our algorithm is *generic* (unifying perspective and orthographic SFS, see section 3). It is very *robust* to pixel noise and errors on the focal length and the position of the light source, and seems to be *the most efficient* SFS (iterative) algorithm so far (see section 5). Also, it can deal with *discontinuous images* and *black shadows* (see section 6).
3. We successfully apply our SFS method to *real images* and we propose *three applications* in three different fields (medical images, document restoration, face reconstruction); see section 7.

## 2 New modeling of the “perspective SFS” problem with a point light source located at the optical center

In this section, we present a new formulation of the “perspective SFS” problem. Among all approaches dealing with “perspective SFS”, only the work of Prados and Faugeras [26], and Tankus et al. [30] proposes a formalism completely based on Partial Differential Equations (PDEs). In this work, the authors assume that the camera performs a perspective projection and that the scene is illuminated by a single point light source *located at infinity*. In this paper, we also model the camera as a pinhole, but we assume that the light source is *located at the optical center*. This model corresponds nicely to the situation encountered in some medical protocols like endoscopy or colposcopy, in which the (point) light source is located very close to the camera, because of space constraints, see section 7.3 for a SFS application in this area. This modeling also corresponds approximately to



$$I(x)\sqrt{f^2|\nabla v(x)|^2 + (\nabla v(x) \cdot x)^2 + Q(x)^2} - Q(x) = 0. \quad (2)$$

To this equation, we associate the *Hamiltonian*

$$H_F(x, p) = I(x)\sqrt{f^2|p|^2 + (p \cdot x)^2 + Q(x)^2} - Q(x).$$

### 3 Unification of the “perspective” and “orthographic SFS”

In this section, we unify various formulations of the SFS problem.

#### 3.1 “Orthographic SFS” with a point light source at infinity

This is the traditional setup for the SFS problem. We denote by  $\mathbf{L} = (\alpha, \beta, \gamma)$  the unit vector representing the direction of the light source ( $\gamma > 0$ ),  $\mathbf{l} = (\alpha, \beta)$ . The function  $S$  parameterizing the surface  $\mathcal{S}$  is given by  $S(x) = (x, u(x))$ . The SFS problem is then, given  $I$  and  $\mathbf{L}$ , to find a function  $u : \bar{\Omega} \rightarrow \mathbb{R}$  satisfying the following brightness equation:

$$\forall x \in \Omega, \quad I(x) = (-\nabla u(x) \cdot \mathbf{l} + \gamma) / \sqrt{1 + |\nabla u(x)|^2},$$

This classical equation has been associated to various Hamiltonians:

1) In [28], Rouy and Tourin introduce

$$H_{R/T}(x, p) = I(x)\sqrt{1 + |p|^2} + p \cdot \mathbf{l} - \gamma.$$

2) In [9], Dupuis and Oliensis consider

$$H_{D/O}(x, p) = I(x)\sqrt{1 + |p|^2} - 2p \cdot \mathbf{l} + p \cdot \mathbf{l} - 1.$$

3) For  $\mathbf{L} = (0, 0, 1)$ , Lions et al. [18] deal with:  $H_{Eiko}(x, p) = |p| - \sqrt{\frac{1}{I(x)^2} - 1}$  (eikonal equation).

#### 3.2 “Perspective SFS” with a point light source at infinity

In [26], Prados and Faugeras parameterize the surface  $\mathcal{S}$  by defining  $S(x) = u(x) (x, -f)$ . Combining the expression of  $\mathbf{n}(x)$  and the change of variables  $v = \ln(u)$ , they obtain from the irradiance equation the following Hamiltonian:

$$H_{P/F}(x, p) = I(x)\sqrt{f^2|p|^2 + (x \cdot p + 1)^2} - (f \mathbf{l} + \gamma x) \cdot p - \gamma;$$

#### 3.3 A generic Hamiltonian

In [25], we prove that all the previous SFS Hamiltonians ( $H_F$ ,  $H_{R/T}$ ,  $H_{D/O}$ ,  $H_{Eiko}$ , and  $H_{P/F}$ ) are special cases of the following “generic” Hamiltonian:

$$H_g(x, p) = \tilde{H}_g(x, A_x p + \vec{v}_x) + \vec{w}_x \cdot p + c_x,$$



with  $\tilde{H}_g(x, q) = \kappa_x \sqrt{|q|^2 + K_x^2}$ ,  
 $\kappa_x, K_x \geq 0$ ,  $A_x = D_x R_x$ ,  $D_x = \begin{pmatrix} \mu_x & 0 \\ 0 & \nu_x \end{pmatrix}$ ,  $R_x$  is the rotation matrix  $\frac{1}{|x|} \begin{pmatrix} x_2 & -x_1 \\ x_1 & x_2 \end{pmatrix}$  if  $x \neq 0$ ,  
 $R_x = Id_2$  if  $x = 0$ ,  $\mu_x, \nu_x \in \mathbb{R}^*$  ( $\mu_x, \nu_x \neq 0$ ),  $\vec{v}_x, \vec{w}_x \in \mathbb{R}^2$  and  $c_x \in \mathbb{R}$ .

By using the Legendre transform, we rewrite this "generic" Hamiltonian as a supremum:

$$H_g(x, p) = \sup_{a \in B_2(0,1)} \{-f_g(x, a) \cdot p - l_g(x, a)\}.$$

In [25], we detail the exact expressions of  $f_g$  and  $l_g$ . This generic formulation considerably simplifies the analysis of the problem. All theorems about the characterization and the approximation of the solutions are proved for this generic SFS Hamiltonian. In particular, this formulation *unifies the orthographic and perspective*<sup>3</sup> SFS problems. Also, from a practical point of view, *a unique code can be used to numerically solve these various problems*.

## 4 A new mathematical framework for SFS without boundary data

It is well-known that the SFS problem is an ill-posed problem. For example, in general, the solution is not unique: several surfaces can yield the same image [10]. So before computing a numerical solution, it is very important to answer the following questions:

Does there exist a solution? If yes, in what sense is it a solution (classical or weak)? Is the solution unique?

The various approaches for providing answers to these questions can be classified in two categories.

**First**, Dupuis and Oliensis [9] characterize the  $C^1$  solutions and Kozera works with hemi-spheres and planes [16]. Nevertheless, we can design smooth images "without (smooth) shape" [2, 17]. This leads to consider the problem in a weaker framework.

**Second**, in the 90s, Lions, Rouy and Tourin [28, 18] propose to solve the SFS problem by using the notion of viscosity solutions. Recently, their approach has been extended by Prados and Faugeras [27, 26] and by Falcone [4, 11].

The theory of viscosity solutions is interesting for a variety of reasons: 1) it ensures the existence of weak solutions as soon as the intensity image is (Lipschitz) continuous; 2) it allows to characterize all solutions; 3) any particular solution is effectively computable. Nevertheless, the work of Lions et al. , Prados and Faugeras, Falcone et al. [28, 18, 27, 26, 4, 11] has a very important weakness: the characterization of a viscosity solution and its computation *require the knowledge of its values on the boundary of the image*. This is *quite unrealistic* because in practice such values are not known.

At the opposite of the work based on the viscosity solutions, Dupuis and Oliensis [9] characterize a  $C^1$  solution by *specifying only its values at the "minimal" critical points*. They do not specify the values of the solution on the boundary of the image.

Considering the advantages and the drawbacks of all these methods, we propose a *new* class of *weak* solutions which guarantees the existence of a solution<sup>4</sup> in a large class of situations including

<sup>3</sup> Including our new model with the light source located at the optical center.

<sup>4</sup>Corresponding to Dupuis and Oliensis'  $C^1$  solution, if one exists.

some where there do not exist smooth solutions. We call these new solutions: “**singular discontinuous viscosity solutions with Dirichlet boundary conditions and state constraints**” (SDVS). This new notion allows to fix the “height” of the solution at the critical points  $\mathcal{S} = \{x \mid I(x) = 1\}$  and on the boundary of the image, when we know it, and allows to “send” these values to infinity when this information is not available (we say that we impose a state constraint). Because of space, refer to [24] for more details. In [24], we prove the *existence* and the *uniqueness* of the SDVS of the SFS equations as soon as the intensity image  $I$  is *Lipschitz continuous and the Hamiltonian is coercive* (e.g.  $H_{D/O}$  and  $H_{R/T}$  are coercive iff  $I(x) > |I|$ ). We also prove the *robustness* of the SDVS solution to *pixel noise* and to *errors in the illumination or focal length parameters*.

## 5 Numerical approximation of the SDVS for the generic SFS problem

This section explains how to compute a numerical approximation of the SDVS of the generic SFS equation. This requires three steps. First we “regularize” the equation. Second, we approximate the “regularized” SFS equation by an approximation scheme. Finally, from the approximation scheme, we design a numerical algorithm.

### 5.1 Regularisation of the generic SFS equation

Given an image  $I$  and  $\varepsilon > 0$ , we note  $I_\varepsilon$  the image<sup>5</sup>  $I_\varepsilon = \min(I, 1 - \varepsilon)$ . By using a stability result, we prove in [24] that for the generic SFS Hamiltonian, the SDVS associated with the image  $I_\varepsilon$  converges uniformly toward the SDVS associated with the image  $I$ , when  $\varepsilon \rightarrow 0$ . Also,  $\forall \varepsilon > 0$ , the generic SFS equation associated with  $I_\varepsilon$  is *not degenerate anymore*. Thus for approximating its solution, we can use the classical tools developed by Barles and Souganidis [1].

### 5.2 An Approximation scheme for the nondegenerate generic SFS equations

Let us consider the “regularised” generic SFS equation. In [1] Barles and Souganidis suggest to consider *monotonous* schemes. So, we construct the following monotonous scheme  $S(\rho, x, u(x), u) = 0$  with

$$S(\rho, x, t, u) = \max_{s_1, s_2 = \pm 1} S_{s_1, s_2}(\rho, x, t, u),$$

where  $\rho = (\Delta x_1, \Delta x_2)$  is the mesh size and where we choose  $S_{s_1, s_2}(\rho, x, t, u) =$

$$\sup_{a \in B_{s_1, s_2}} \left\{ -f_g(x, a) \cdot \left( \frac{t - u(x + s_1 \Delta x_1 \vec{e}_1)}{-s_1 \Delta x_1} \right) - l_g(x, a) \right\}.$$

$B_{s_1, s_2} = \{a \in B(0, 1) \mid f_{g_1}(x, a)_{s_1} \geq 0 \text{ and } f_{g_2}(x, a)_{s_2} \geq 0\}$ .  
(reminder:  $f_g$  and  $l_g$  are defined in section 3.3).

<sup>5</sup>We assume that the intensity is between 0 and 1.

Using Barles and Souganidis definitions [1], we prove that this scheme is always monotonous and stable. Also, it is *consistent* with the generic SFS Hamiltonian as soon as the image is Lipschitz continuous. Finally we prove that, if furthermore the Hamiltonian is coercive in  $p$ , then the solution of the scheme, noted  $w^\rho$ , *converge toward the unique SDVS* of the “regularized” generic SFS equation, when the mesh size vanishes to zero.

### 5.3 Numerical algorithms for the generic SFS problem

In the previous section, we have proposed a scheme whose solutions converge toward the unique SDVS of the “regularized” generic SFS equation. We now describe an algorithm that computes a numerical approximation of the solution of the scheme.

For a fixed mesh size  $\rho = (\Delta x_1, \Delta x_2)$ , let us denote  $x_{ij} := (i\Delta x_1, j\Delta x_2)$ . The algorithm consists of the following computation of the sequence of values  $U_{ij}^n$ ,  $n \geq 0$  ( $U_{ij}^n$  being an approximation of  $w^\rho(x_{ij})$ ).

- Algorithm :**
- 1) Initialisation ( $n = 0$ ):  $U_{ij}^0 = u_0(x_{ij})$ .
  - 2) Choice of a pixel  $x_{ij} \in \Omega$  and modification of  $U_{ij}^n$ :  
 We choose  $U^{n+1}$  such that  $\forall (k, l) \neq (i, j)$ ,  
 $U_{kl}^{n+1} = U_{kl}^n$  and  $S(\rho, x_{ij}, U_{ij}^{n+1}, U^n) = 0$ .
  - 3) Choose the next pixel  $x_{ij} \in \Omega$  in such a way that all pixels of the image are regularly visited and go back to 2.

We prove in [25] that if  $u_0$  is a supersolution, then the computed numerical approximations converge toward a solution of the scheme. In [26], Prados and Faugeras use the same algorithm (for the particular Hamiltonian  $H_{P/F}$ ), starting from a subsolution. When we start from a supersolution, we reduce the number of iterations by 3 orders of magnitude! In [26], the authors need around 4000 iterations for computing the surface of the classical Mozart’s face [34]. Starting from a supersolution (in practice, a large constant function  $u_0$  with the appropriate boundary data does the trick!), *only four iterations are sufficient* for obtaining a good result, see figure 2. Moreover, in [25], we show some comparisons of our results with those of what we consider to be the most efficient (orthographic) iterative algorithm of the SFS literature [9]. After the same number of iterations, the results obtained with our algorithm are slightly better visually than those obtained by the algorithm of [9]. This is confirmed quantitatively by the computation of the classical  $L_1$ ,  $L_2$  and  $L_\infty$  errors. Nevertheless let us note that the cost of one update is slightly larger for our (implicit) algorithm than for the (semi-implicit) algorithm of [9]. This may also be because we have not optimized our code for this special case. Because of space, we do not detail and display the results of these comparisons. Let us emphasize again that the SDVS method does not necessarily require boundary data. For example, figure 2 shows some reconstructions of the Mozart face with no boundary data, except for the tip of the nose. Moreover, as predicted by the theory, our algorithm shows an exceptional robustness to noise and errors on the parameters. This robustness is even bigger when we send the boundary to infinity (apply the state constraints). Figure 2-d) displays a reconstruction of Mozart’s face from the noisy image c) (additive uniformly distributed white noise [SNR  $\simeq$  5]) with our generic algorithm

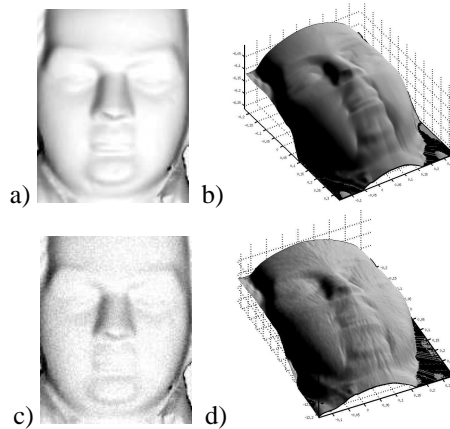


Figure 2: a) *Perspective* synthetic image generated from the classical Mozart's face [34] [size  $\simeq 130 \times 170$ ,  $\mathbf{L} = (0.1, 0.3, 0.85)$ ,  $f = 5$ ]; b) reconstructed surface from a) by our generic algorithm after 4 iterations; c) noisy image ( $SNR \simeq 5$ ); d) reconstructed surface from c) by our generic algorithm after 4 iterations with the wrong parameters  $\mathbf{L}_\epsilon = (0.2, 0.2, 0.96)$ ,  $f_\epsilon = 10$  (the error angle  $(\mathbf{L}_\epsilon, \mathbf{L})$  is  $\simeq 9^\circ$ ).

provided with wrong parameters for the focal length and for the light direction. Finally, let us remark that our algorithm computes numerical approximations of the *SDVS generic* SFS problem. Thus, we only need to implement a *single* algorithm for all SFS models (at the cost of a small decrease in efficiency).

More details can be found in [25, 24] which also contains the proofs of all our statements.

## 6 A SFS method dealing with discontinuous images and black shadows

Among all the difficulties encountered when attempting to solve the SFS problem, the intensity discontinuities such as those caused by black shadows are among the most difficult to deal with.

The discontinuities of an image<sup>6</sup> are generally caused by edges, black shadows and occluding contours. At the opposite of the classical point of view (see e.g. the work of Malik and Maydan [19]), the notion of viscosity solutions provides a natural framework for dealing with non smooth surfaces<sup>7</sup> (and with edges). Nevertheless, *the theory of the viscosity solutions does not yet apply to discontinuous images*<sup>8</sup> (and hence to black shadows). So, for dealing with black shadows, Lions et al. [18] do not “recover” surfaces in the areas of 0 intensity and pose the problem in terms of boundary conditions. Recently, Falcone et al. [11] noted that, in the black shadows areas, the surface formed by the rays of light grazing the solution, verify the irradiance equation. Thus, for recovering

<sup>6</sup>generated from a scene with a constant albedo.

<sup>7</sup>Viscosity solutions are *weak* (i.e. non differentiable) solutions.

<sup>8</sup>Most probably, some recent work [23, 15, 29] on the Eikonal equation will shortly allow to extend the theory.

a solution, we do not need to separate the “shading areas” and the “shadow areas”. Also, in general<sup>9</sup>, our generic algorithm returns approximations of the exact solutions in shading areas and returns the grazing rays of light in the black shadows areas (as does the algorithm proposed by Falcone [11] for the “orthographic SFS”), thereby providing a satisfying numerical solution. Moreover<sup>10</sup>, we prove that our *generic approximation scheme is stable* and that the *numerical solutions computed by our generic algorithm converge, even when the image contains discontinuities and black shadows*. Figure 3 illustrates the ability of our generic numerical algorithm to deal with *black shadows*.

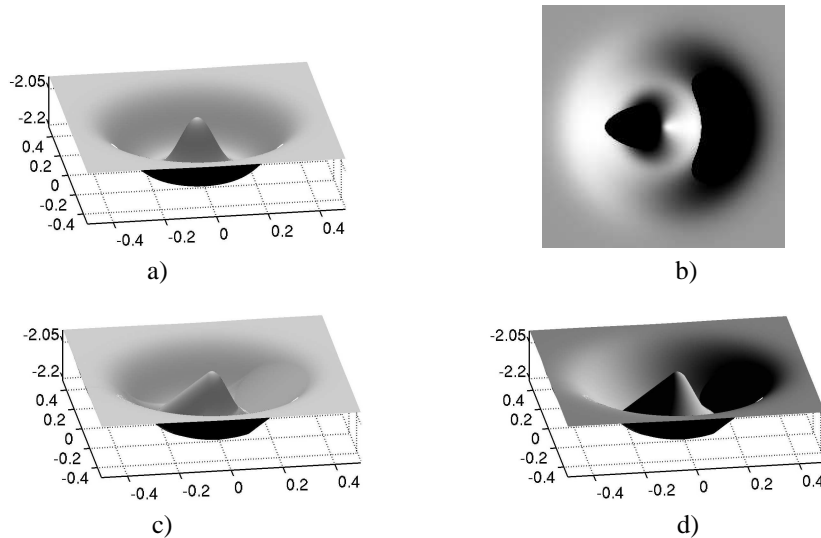


Figure 3: Example of a reconstruction from a synthetic image with black shadows. a) Original surface (illuminated by a vertical light); b) Synthetic image computed from the surface a) with  $\mathbf{L} = (0.8, 0.0, 0.6)$  [ $(\mathbf{L}, \vec{Oz}) = 53^\circ$ ]; c) Solution recovered by our algorithm from the image b) (illuminated by a vertical light); d) Surface c) illuminated by the light used for image b).

## 7 Toward applications of Shape from Shading

In this section, we suggest some *applications* of our SFS method. Because of space, we do not provide complete descriptions, but we hope that the results will convince the reader of the *applicability of our SFS method to real problems*. Let us emphasize that all the results we present in this section are obtained from real images:

**Note:** When we apply SFS methods to real images we assume that the camera is geometrically

<sup>9</sup> If we assume that the critical points and the boundary of the image are not covered by the shadows.

<sup>10</sup> although the theory of viscosity solutions does not yet apply,

and photometrically calibrated. In our experiments of sections 7.1 and 7.2 we know the focal length (5.8 mm) and approximately the pixel size (0.0045 mm; CCD size = 1/2.7") of our cheap digital camera (Pentax Optio 330GS). In section 7.3, we choose some arbitrary reasonable parameters. Also, note that there exist classical methods to calibrate photometrically a camera [20, 21]. In our tests, we do not use them, but we make some educated guesses for gamma correction (when the photometric properties of the images seem incorrect).

## 7.1 Document restoration using SFS

In this section, we propose a *reprographic system*<sup>11</sup> to remove the geometric and photometric distortions generated by the classical photocopy of a bulky book. A first solution has been proposed by Wada and coworkers [32] who deal with *scanner* images involving a complex optical system (with a moving light). Here, the acquisition process we use is a classical camera<sup>12</sup>. The book is illuminated by a single light source located at infinity or close to the optical center (following the models we describe in sections 2 and 3). Note that Cho et al. [5] propose a similar system but they use two light sources<sup>13</sup>. The acquired images are then processed using our SFS method to obtain the shape of the photographed page. Let us emphasize that, for obtaining a compact experimental system, the camera must be located relatively close to the book. Therefore the *perspective model is especially relevant* for this application. Also, the distortion due to the perspective clearly appears in the image c) of figure 4.

In our SFS method we assume that the albedo is constant. In this application, this does not hold because of the printed parts. Before recovering the surface of the page, we therefore localize the printed parts by using image statistic (similar to Cho's [5]) and we erase them automatically by using e.g. the inpainting algorithm of Tschumperle and Deriche [31]. This step can produce an important pixel noise. Nevertheless, this is not a problem for us because, as figure 4-b) shows, *our SFS method is extremely robust to pixel noise*: figure 4-b) displays the result produced by our algorithm (after 10 iterations) using the image of a text page with its pigmented parts, Fig.4-a). In this test, characters are considered as noise. Note that one could say that such a restoration system (based on SFS) is flawed because it does not use the information provided by the *rows* of characters. This is partially true but nevertheless, for pages containing few rows of characters but a lot of graphics and pictures (separated by large white bands<sup>14</sup>), such a SFS method could provide a simple and efficient solutions.

Once we have recovered the three-dimensional shape of the page, we can flatten the surface by using e.g. the algorithm of Brown and Seales<sup>15</sup> [3]. Note that at each step of this restoration process (3D reconstruction and flattening) we keep the correspondences with the pixels in the image. Thus, at the final step, we can restore the printed parts.

To prove the applicability of this method, we have tested it on a page mapped on a cylindrical sur-

---

<sup>11</sup>Suggested to us by Durou (private communication, [7]).

<sup>12</sup>Note that a camera snapshot is practically instantaneous, whereas a scan takes several seconds.

<sup>13</sup>We can also note that the numerical method proposed by [5] requires that global variations of depth only exist along one direction. Our method does not require this hypothesis.

<sup>14</sup>This is often the case for scientific documents.

<sup>15</sup>Not yet implemented, because of time.

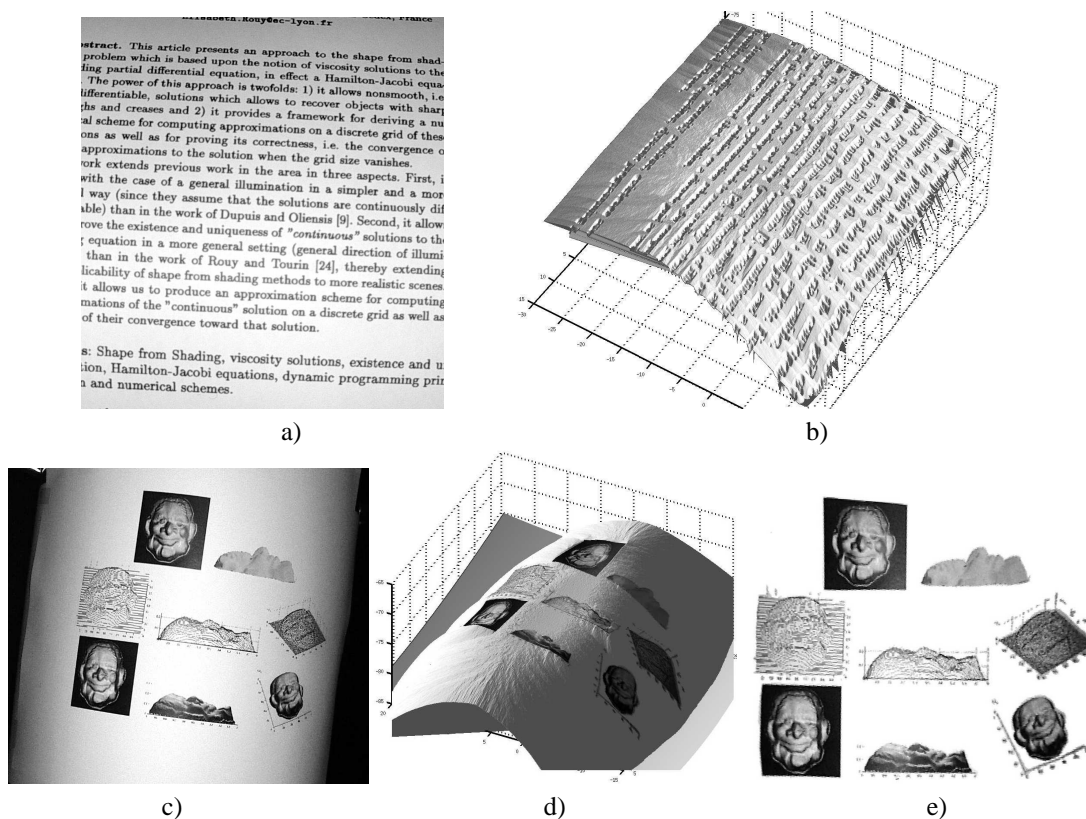


Figure 4: a) Real image of a page of text [size  $\simeq 800 \times 800$ ]; b) Surface recovered from a) by our generic algorithm (without removing the printed parts of a)), c) real image of a page containing pictures and graphics [size  $\simeq 2000 \times 1500$ ], d) surface (textured by the printed parts of c)) recovered from c) by our generic algorithm (after having removed and inpainted the ink parts of c)). e) An orthographic projection of the surface d): the geometric (and photometric) distortions are significantly reduced.

face<sup>16</sup> (we have used our cheap camera and flash in an approximately dark room). Figure 4 shows the original image in c), the reconstructed surface (after 10 iterations) (textured by the ink parts of c)) in d) and an orthographic projection of the reconstructed surface, in e). Figure 4-e) indicates that our method allows to remove the perspective and photometric distortions.

## 7.2 Face reconstruction from SFS

The interest of the SFS methods for some applications dealing with faces has been demonstrated in e.g. the work of Zhao and Chellappa [35] (who use symmetric SFS for illumination-insensitive face recog-

<sup>16</sup>For emphasizing the perspective effect.

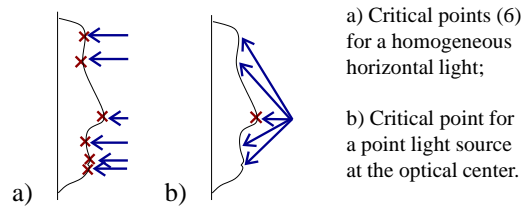


Figure 5: Critical points of the profile of a face.

dition), and by Choi and coworkers [6] (who use SFS for determining the face pose). In this section we propose a very simple protocol based on SFS for face reconstruction. We use one camera equipped with a basic flash in an approximately dark place. As shown in figure 5, the interest of this method lies in the fact that, with such a protocol, the generated image should contain a unique critical point (if the distance of the face to the camera and the focal length are sufficiently small). Therefore, the propagation of the height information starts from this unique critical point.

We have tested our generic algorithm on a real image of a face<sup>17</sup> located at  $\simeq 700$  mm of the camera in an approximately dark place (see Fig.6-a)). Figure 6-b,c,d) shows the surfaces recovered by our generic algorithm (after 5 iterations) with the orthographic model ( $\mathbf{L} = (0, 0, 1)$ ), with the perspective model using a point light source at infinity in the direction ( $\mathbf{L} = (0, 0, 1)$ ), and with the perspective model with a point light source at the optical center, respectively<sup>18</sup>.

As in the previous application, the albedo is not constant over the whole image. Therefore we removed the eyes and the eyebrows in the image by using e.g. the inpainting algorithm of Tschumperle and Deriche [31]. Moreover, note that this step can be automated by matching the image<sup>19</sup> to a model image already segmented. Figure 6 shows in e) the surface recovered from the image obtained after the inpainting process.

### 7.3 Potential applications to medical images

In this section, we are interested in applying our SFS method to some medical images. Our interest is motivated by the work of Craine et al. [8] (who use SFS for correcting some errors on the quantitative measurement of areas in the cervix, from colposcopy images) and by the work of Yamany et al. [33] (who propose a system based on SFS for human jaw modeling using intra-oral images). For illustrating the relevance of the “perspective SFS” modeling with the light source located at the optical center, we apply our algorithm to an endoscopic image of a normal stomach<sup>20</sup> (see figure 7-a)). In fact, for producing such an image, the light source must be very close to the camera, because of space constraints. In figure 7-b-c-d), we show the results obtained (after 3 iterations) by our generic algorithm in the orthographic case ( $\mathbf{L} = (0, 0, 1)$ ), in the perspective case with the light source at infinity ( $\mathbf{L} = (0, 0, 1)$ ) and in the perspective case with the light source at the optical center, respectively<sup>18</sup>. In figure 7-

<sup>17</sup>Slightly made-up to be more Lambertian.

<sup>18</sup>The parameters used for the focal length and the pixel size are the same in the three cases.

<sup>19</sup>We can use for example the very robust multi-modal and non-rigid matching method proposed by Hermosillo and Faugeras in [12].

<sup>20</sup>Suggested by Tankus and Sochen (private communication) and downloaded from <http://www.gastrolab.net/>.



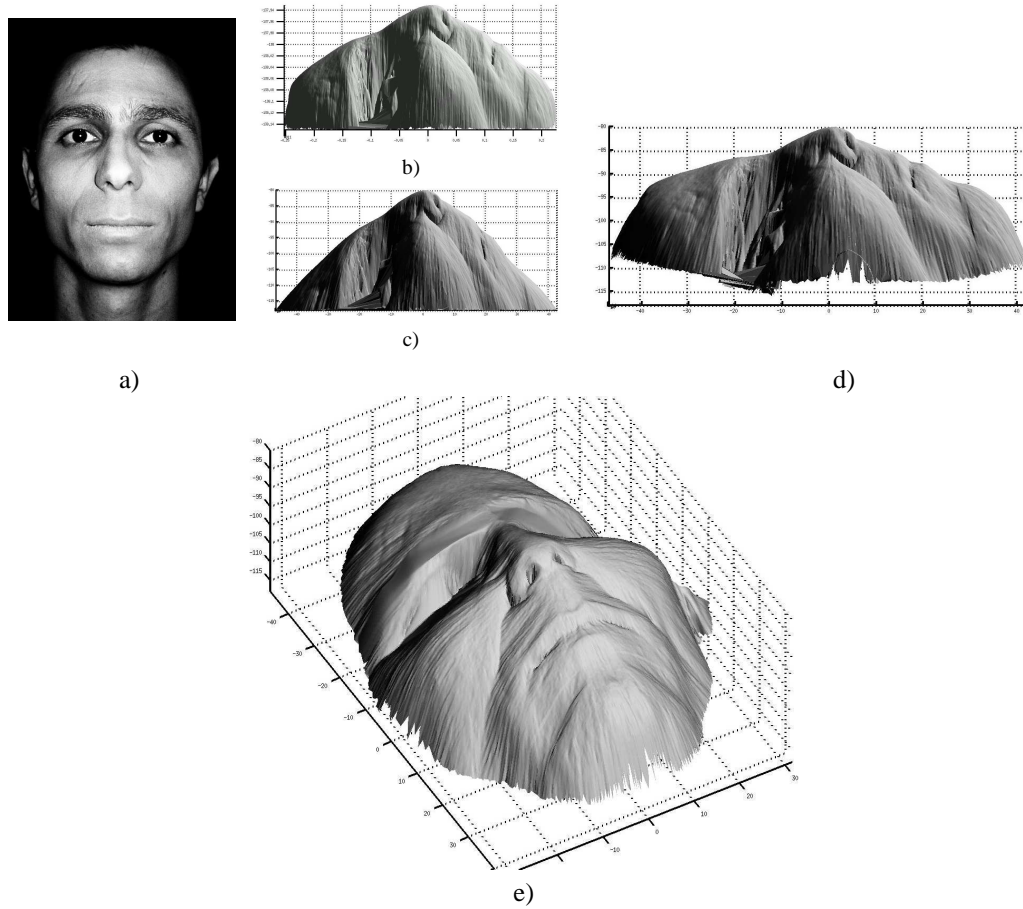


Figure 6: a) Real face image [size  $\simeq 450 \times 600$ ]; b) surface recovered from a) by our generic algorithm with the orthographic model ( $\mathbf{L} = (0, 0, 1)$ ); c) surface recovered from a) by our generic algorithm with the perspective model with the light source at infinity ( $\mathbf{L} = (0, 0, 1)$ ); d) surface recovered from a) by our generic algorithm with the perspective model with the light source located at the optical center; e) surface recovered by our generic algorithm with the same modeling hypotheses as d) after the inpainting process.

b-c-d), the surfaces are visualized from the same point of view with a light source located at the optical center. These three reconstructions look quite good. To further show the quality of the last reconstruction, we display the surface d) with a different illumination. Let us emphasize that the reconstruction d) based on the perspective model with the light source at the optical center, is *globally convex*. Therefore it is *more realistic* than the other two reconstructions (based on incorrect models) which are *globally concave*.

Finally, notice that the stomach wall is not perfectly Lambertian (see Fig.7-a)). This suggests the robustness of our SFS method to departures from the Lambertian hypothesis.

## 8 Conclusion

We have proposed a new method, firmly grounded in mathematics, for solving the SFS problem under much more realistic hypotheses than in previous work. This method allows us to prove the existence and uniqueness of a solution of the SFS problem. This solution does not have to be smooth everywhere, in agreement with the shapes of many real objects and their images which can contain strong shadows. Its existence does not require the knowledge of unrealistic boundary conditions but this knowledge can be used, when available. We have designed a provably convergent algorithm for computing these solutions which is very robust to pixel noise and errors on such parameters as light source position, focal length and albedo. This algorithm is generic, and deals with discontinuous images and black shadows. We have successfully applied our SFS method to real images and we have suggested that it may be useful in a number of real-life applications.

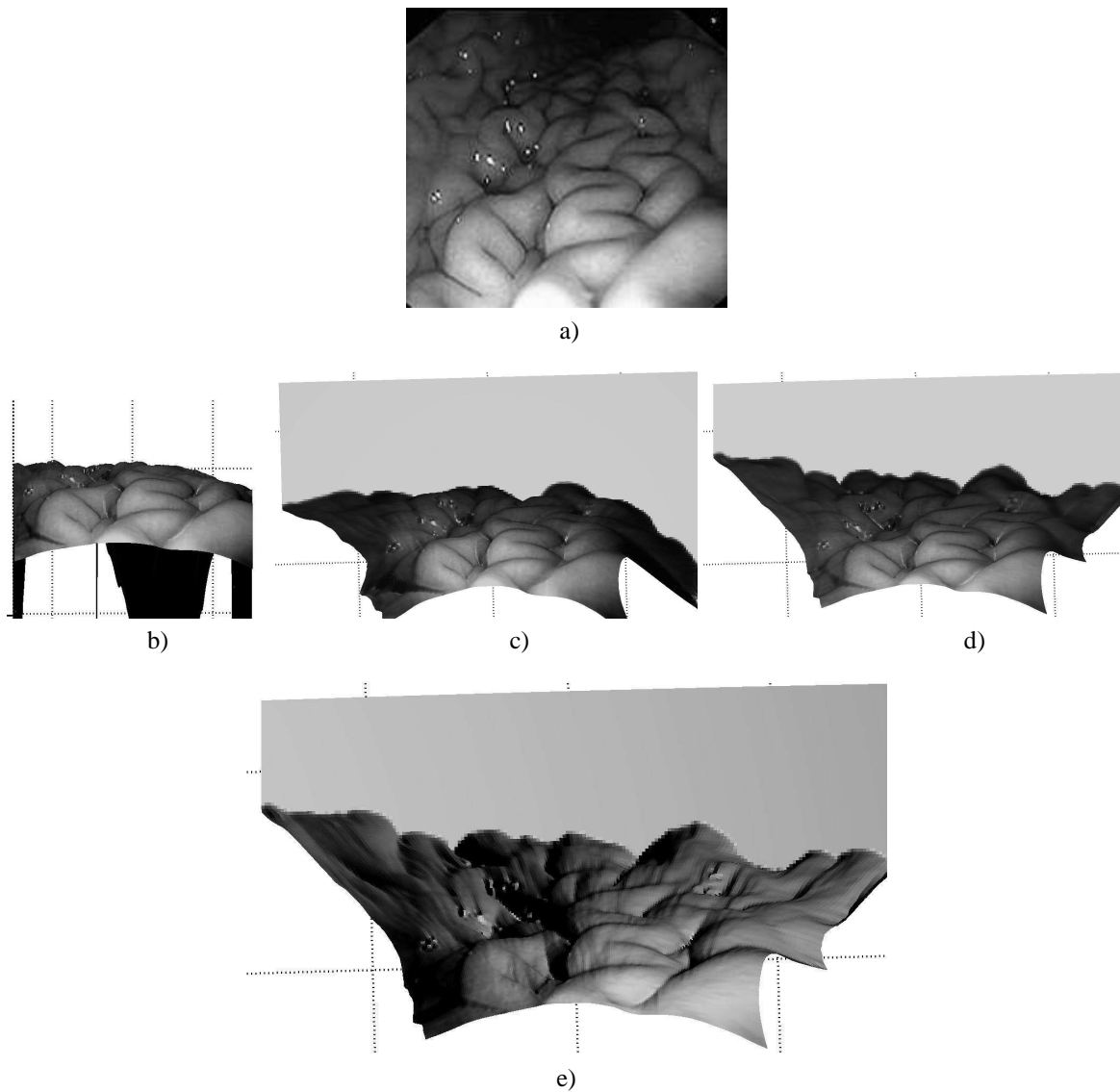


Figure 7: Reconstruction of a normal stomach: a) Original image of a normal stomach [size  $\simeq 200 \times 200$ ]; b) surface recovered from a) by our generic algorithm with the orthographic model ( $\mathbf{L} = (0, 0, 1)$ ); c) surface recovered from a) by our generic algorithm with the perspective model with the light source at infinity ( $\mathbf{L} = (0, 0, 1)$ ); d) surface recovered from a) by our generic algorithm with the perspective model and with the light source located at the optical center; e) surface d) visualized with a different illumination.

## References

- [1] G. Barles and P.E. Souganidis. Convergence of approximation schemes for fully nonlinear second order equations. *Asymptotic Analysis*, 4:271–283, 1991.
- [2] M.J. Brooks, W. Chojnacki, and R. Kozera. Shading without shape. *Quarterly of Applied Mathematics*, 50(1):27–38, 1992.
- [3] M. S. Brown and W. B. Seales. Document restoration using 3D shape. In *Proceedings of ICCV'01*, July 2001.
- [4] F. Camilli and M. Falcone. An approximation scheme for the maximal solution of the shape-from-shading model. *International Conference on Image Processing*, pages 49–52, 1996.
- [5] S.I. Cho and H. Saito. A Divide-and-Conquer Strategy in Shape from Shading problem. In *Proceedings of CVRP'97*, June 1997.
- [6] K.N. Choi, P. Worthington, and E.R. Hancock. Facial pose using shape-from-shading. In *Proceedings of BMVC'99*, pages 402–411, 1999.
- [7] F. Courteille, A. Cruzil, J.-D. Durou, and P. Gurdjos. Shape from Shading en conditions réalistes d'acquisition photographique. In *Proceedings of RFIA'04*, 2004.
- [8] B.L. Craine, Craine E.R., C.J. O'Toole, and Q. Ji. Digital imaging colposcopy: Corrected area measurements using Shape-from-Shading. *IEEE Transactions on Medical Imaging*, 17(6):1003–1010, December 1998.
- [9] P. Dupuis and J. Oliensis. An optimal control formulation and related numerical methods for a problem in shape reconstruction. *The Annals of Applied Probability*, 4(2):287–346, 1994.
- [10] J.-D. Durou and D. Piau. Ambiguous shape from shading with critical points. *Journal of Mathematical Imaging and Vision*, 12(2):99–108, 2000.
- [11] M. Falcone, M. Sagona, and A. Seghini. A scheme for the shape-from-shading model with "black shadows". In *Proceedings of ENUMATH 2001*, 2001.
- [12] G. Hermosillo and O. Faugeras. Dense image matching with global and local statistical criteria: a variational approach. In *Proceedings of CVPR'01*, 2001.
- [13] B.K.P. Horn. Obtaining shape from shading information. In P.H. Winston, editor, *The Psychology of Computer Vision*. McGraw-Hill, New York, 1975.
- [14] IEEE Computer Society. Nice, France, 2003. IEEE Computer Society Press.
- [15] J. Kain and D.N. Ostrov. Numerical shape-from-shading for discontinuous photographic images. *The International Journal of Computer Vision*, 44(3):163–173, 2001.

- 
- [16] R. Kozera. Uniqueness in shape from shading revisited. *International Journal of Mathematical Imaging and Vision*, 7:123–138, 1997.
- [17] R. Kozera. An overview of the shape from shading problem. *Machine Graphics and Vision*, 7(1-2):291–312, 1998.
- [18] P.-L. Lions, E. Rouy, and A. Tourin. Shape-from-shading, viscosity solutions and edges. *Numer. Math.*, 64:323–353, 1993.
- [19] J. Malik and D.E. Maydan. Recovering three-dimensional shape from a single image of curved objects. *IEEE Transactions on Pattern Analysis and Machine Intelligence*, 11(6):555–566, 1989.
- [20] C.S. McCamy, H. Marcus, and J.G. Davidson. A colorrendition chart. *J. App. Photog. Eng.*, 2:95–99, 1976.
- [21] G.W. Meyer. Wavelength selection for synthetic image generation. *Computer Vision, Graphics, and Image Processing*, 41:57–79, 1988.
- [22] J. Oliensis. Shape from shading as a partially well-constrained problem. *CVGIP: Image Understanding*, 54(2):163–183, 1991.
- [23] D.N. Ostrov. Extending viscosity solutions to eikonal equations with discontinuous spatial dependence. *Nonlinear Anal.*, 42(4):709–736, 2000.
- [24] E. Prados, F. Camilli, and O. Faugeras. A viscosity method for Shape from Shading without boudary data. Technical report, INRIA, To appear in 2004.
- [25] E. Prados and O. Faugeras. A mathematical and algorithmic study of the lambertian SFS problem for orthographic and pinhole cameras. Technical Report RR-5005, INRIA, November 2003.
- [26] E. Prados and O. Faugeras. “Perspective Shape from Shading” and viscosity solutions. In *Proceedings of the 9th International Conference on Computer Vision* [14], pages 826–831.
- [27] E. Prados, O. Faugeras, and E. Rouy. Shape from shading and viscosity solutions. In A. Heyden, G. Sparr, M. Nielsen, and P. Johansen, editors, *Proceedings of the 7th European Conference on Computer Vision*, volume 2351, pages 790–804, Copenhagen, Denmark, May 2002. Springer-Verlag.
- [28] E. Rouy and A. Tourin. A Viscosity Solutions Approach to Shape-from-Shading. *SIAM Journal of Numerical Analysis*, 29(3):867–884, June 1992.
- [29] P. Soravia. Optimal control with discontinuous running cost: eikonal equation and shape from shading. In *39th IEEE Conference on Decision and Control*, pages 79–84, December 2000.
- [30] A. Tankus, N. Sochen, and Y. Yeshurun. A new perspective [on] Shape-from-Shading. In *Proceedings of the 9th International Conference on Computer Vision* [14], pages 862–869.

- 
- [31] D. Tschumperlé and R. Deriche. Vector-valued image regularization with PDE's : A common framework for different applications. In *IEEE Conference on Computer Vision and Pattern Recognition*, Madison, Wisconsin (United States), June 2003.
  - [32] T. Wada, H. Ukida, and T. Matsuyama. Shape from shading with interreflections under proximal light source-3D shape reconstruction of unfolded book surface from a scanner image. In *Proceedings of ICCV'95*, June 1995.
  - [33] S.M. Yamany and A.A. Farag. A system for human jaw modeling using intra-oral images. In *IEEE-EMBS*, volume 20, pages 563–566, 1998.
  - [34] R. Zhang, P.-S. Tsai, J.-E. Cryer, and M. Shah. Shape from Shading: A survey. *IEEE Transactions on Pattern Analysis and Machine Intelligence*, 21(8):690–706, August 1999.
  - [35] W. Zhao and R. Chellappa. Illumination-insensitive face recognition using symmetric Shape-from-Shading. In *proceedings of CVPR'00*, pages 1286–1293, 2000.

## Contents

<b>1</b>	<b>Introduction</b>	<b>3</b>
<b>2</b>	<b>New modeling of the “perspective SFS” problem with a point light source located at the optical center</b>	<b>3</b>
<b>3</b>	<b>Unification of the “perspective” and “orthographic SFS”</b>	<b>5</b>
3.1	“Orthographic SFS” with a point light source at infinity . . . . .	5
3.2	“Perspective SFS” with a point light source at infinity . . . . .	5
3.3	A generic Hamiltonian . . . . .	5
<b>4</b>	<b>A new mathematical framework for SFS without boundary data</b>	<b>6</b>
<b>5</b>	<b>Numerical approximation of the SDVS for the generic SFS problem</b>	<b>7</b>
5.1	Regularisation of the generic SFS equation . . . . .	7
5.2	An Approximation scheme for the nondegenerate generic SFS equations . . . . .	7
5.3	Numerical algorithms for the generic SFS problem . . . . .	8
<b>6</b>	<b>A SFS method dealing with discontinuous images and black shadows</b>	<b>9</b>
<b>7</b>	<b>Toward applications of Shape from Shading</b>	<b>10</b>
7.1	Document restoration using SFS . . . . .	11
7.2	Face reconstruction from SFS . . . . .	12
7.3	Potential applications to medical images . . . . .	13
<b>8</b>	<b>Conclusion</b>	<b>15</b>



---

Unité de recherche INRIA Sophia Antipolis  
2004, route des Lucioles - BP 93 - 06902 Sophia Antipolis Cedex (France)

Unité de recherche INRIA Futurs : Parc Club Orsay Université - ZAC des Vignes  
4, rue Jacques Monod - 91893 ORSAY Cedex (France)

Unité de recherche INRIA Lorraine : LORIA, Technopôle de Nancy-Brabois - Campus scientifique que  
615, rue du Jardin Botanique - BP 101 - 54602 Villers-lès-Nancy Cedex (France)

Unité de recherche INRIA Rennes : IRISA, Campus universitaire de Beaulieu - 35042 Rennes Cedex (France)

Unité de recherche INRIA Rhône-Alpes : 655, avenue de l'Europe - 38334 Montbonnot Saint-Ismier (France)

Unité de recherche INRIA Rocquencourt : Domaine de Voluceau - Rocquencourt - BP 105 - 78153 Le Chesnay Cedex (France)

---

Éditeur  
INRIA - Domaine de Voluceau - Rocquencourt, BP 105 - 78153 Le Chesnay Cedex (France)

<http://www.inria.fr>

ISSN 0249-6399